

Molecular fluorescence at a rough surface: The orientation effects

W. L. Blacke and P. T. Leung*

*Department of Physics and Environmental Science and Resources Program,
Portland State University, P.O. Box 751, Portland, Oregon 97207-0751*

(Received 24 April 1997)

The problem of the dynamical interaction between an emitting dipole and a metallic grating surface is considered with particular interest in the effects due to different orientations of the dipole with respect to the substrate surface. Our previous perturbative theory is extended to treat both parallel and perpendicular dipoles and the results are applied to the study of modified fluorescence characteristics for admolecules in the vicinity of a rough metal surface modeled as a grating. Numerical results show that some of the characteristics are very sensitive to the molecular orientation and the one along the grating direction is manifested with some unique behavior. The possibility of lengthening molecular lifetimes at a patterned surface is indicated via the manipulation of the surface roughness as well as the orientations of the molecules. In addition, the limitation of the usual step in averaging the theoretical results in the comparison with experimental measured values is pointed out. [S0163-1829(97)08843-7]

I. INTRODUCTION

There has been considerable interest in the study of fluorescence of molecules (e.g., dyes) in the vicinity of a metal surface since the early 1970s.¹⁻³ Experimental measurements of various fluorescence characteristics (e.g., lifetimes) were achieved for both the far-distance (with molecule-surface distance $d \geq 10$ nm)^{1,2} and the close-distance ($d \leq 10$ nm) regimes.⁴ Theoretically, there have been both classical and quantum-mechanical approaches in the calculation of these modified characteristics.⁵ Among the many theories, one of the most efficient approaches was the classical phenomenological model accomplished mainly by Chance, Prock, and Silbey³ (CPS) which has accounted successfully for many of the “far-distance” experimental results. In the CPS theory, the fluorescing molecule is modeled as an emitting point dipole with its emission characteristics modified by the field (E') reflected from the substrate surface. The full electrodynamics are then solved with the application of the Sommerfeld theory.⁶ The frequency shifts and modified decay rates (normalized to the free molecule value) can then be obtained as follows:

$$\frac{\Delta\omega}{\gamma_0} = \frac{-3q}{4\mu k^3} \operatorname{Re}E', \quad (1)$$

$$\frac{\gamma}{\gamma_0} = 1 + \frac{3q}{2\mu k^3} \operatorname{Im}E', \quad (2)$$

where μ is the dipole moment, q the intrinsic quantum yield, and k the emission wave number of the admolecule. Note that, strictly speaking, the CPS theory is limited to the surface of perfect flatness, which can be a reasonable idealization in actual experiments for molecules at large distances from a well-prepared surface. It was the observation in the 1980s of deviations from the CPS theory at close molecule-surface distances⁴ that led to a series of studies on the corrections to the CPS theory due to surface roughness.⁷⁻¹¹ In particular, both the static (image)^{7,8} and the more exact

dynamic⁹⁻¹¹ theories have been considered for both random⁷ and periodic⁸⁻¹¹ roughness in the literature. For perpendicularly oriented molecular dipoles, the previous works have indicated that surface roughness can either enhance or suppress the effects from a flat surface, and can lead to extra morphology-induced resonances in the decay rate spectrum of the admolecules.

It is the purpose of the present work to enlarge the previous dynamical theory⁹ for the interaction of an emitting dipole with a rough surface (modeled as a grating) allowing the dipole to have an arbitrary orientation with respect to the rough surface. The results will be applied to study the effects on the modified fluorescence characteristics due to the different orientations of the admolecules. Our paper is organized as follows. We start in Sec. II with a brief summary and further clarification of our previous perturbative method in calculating the reflected field E' from a rough boundary. We then present in Sec. III our results for the various fluorescence characteristics for both the perpendicular and parallel dipoles and shall compare them with those from the static theory. Numerical illustrations for a silver grating substrate will be shown in Sec. IV and conclusion in Sec. V. Among other implications from our results, we shall see that the usual step in “averaging the molecular orientations” for a randomly oriented ensemble of admolecules must be handled with care in the case of patterned substrate surfaces.

II. A DYNAMICAL PERTURBATION THEORY

The problem we are going to model in this section involves the dynamical interaction between an oscillating point dipole (in vacuum) with a semi-infinite substrate grating surface as depicted in Fig. 1. For the case with a dipole moment (μ) perpendicular (along z) to the substrate surface, the problem has been solved previously in a perturbative approach in both a dynamic⁹ and a simpler static⁸ approach via the application of the image theory (IT). For the case of an arbitrarily oriented dipole, only IT has been carried out in the previous investigations by deriving results for the two cases

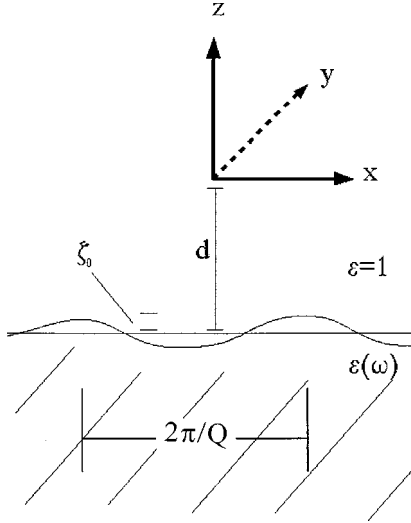


FIG. 1. The geometry of the dipole-substrate system. The dipole orientations and distance are shown, along with the dielectric constants and roughness parameters of the substrate.

with parallel oriented dipoles (along x and y , respectively). It is well established that IT is accurate only when (1) the molecular dipole is located at a distance (d) much smaller than its emission wavelength, (2) the substrate conductivity is not too high so that $d \lesssim \delta$, the skin depth of the metal substrate, and (3) the emission frequency is not close to the morphology-induced resonance frequency for resonant radiative energy transfer to take place.¹² Hence, to obtain a model that can study the orientation effects more accurately, it is our purpose here to generalize our previous dynamical theory⁹ to cases with molecular orientations parallel to the plane of the substrate surface. As is clear from Eqs. (1) and (2), the main quantity we have to calculate in order to determine the modified emission characteristics for the admolecules is the reflected field from the rough substrate surface acting at the dipole site. To solve the electrodynamic (Maxwell) equations in a perturbative approach with the roughness as perturbation parameters, we have previously⁹ followed the original Green-function formulation of Maradudin and Mills¹³ (MM) with modifications from the work of Agarwal.¹⁴ In the following, we shall first recapitulate and clarify some of the essence in the MM theory as applied to our dipole-substrate problem before we present the complete set of expressions for the fluorescence characteristics in the next section. We shall limit ourselves to first-order perturbation and hence the degree of roughness is assumed to be small throughout the present work.

By implementing a Born-type approximation scheme, MM were able to obtain the μ th component of the reflected field due to roughness to the first order in the roughness amplitude in the following form:

$$E_{\mu}^{rR} = -\frac{k^2}{16\pi^3} (\varepsilon - 1) \int d^2\mathbf{k}_{\parallel} e^{i\mathbf{k}_{\parallel} \cdot \mathbf{r}_{\parallel}} \hat{\xi}(\mathbf{k}_{\parallel} - \mathbf{k}_{\parallel}^{(0)}) \times \int dz' d_{\mu\nu}(\mathbf{k}_{\parallel}, \omega|zz') \delta(z') E_{\nu}^{(0)}(\mathbf{k}_{\parallel}^{(0)}, \omega|z'), \quad (3)$$

where $\mathbf{k}_{\parallel} = (k_x, k_y, 0)$, $\mathbf{r}_{\parallel} = (x, y, 0)$, and $\hat{\xi}$ is the two-dimensional (2D) Fourier transform of the surface profile

function. $E^{(0)} = E^{\text{in}} + E^{rF}$ is the total field (incident+reflected) in the case of flat surface and $d_{\mu\nu}$ is the Green dyadic function as given in the original MM paper.¹³ Strictly speaking, Eq. (3) is valid only for the case of a plane incident wave with a constant $\mathbf{k}_{\parallel}^{(0)}$ vector, so that $E^{(0)}(\mathbf{k}_{\parallel}^{(0)}, \omega|z') = e^{i\mathbf{k}_{\parallel}^{(0)} \cdot \mathbf{r}} E^{(0)}(\omega|z')$. For a dipole emission as the incident source, a full 2D Fourier transform has to be applied for $E^{(0)}$ to sum over all possible $\mathbf{k}_{\parallel}^{(0)}$ and Eq. (3) has to take the following form:

$$E_{\mu}^{rR} = -\frac{k^2}{16\pi^3} (\varepsilon - 1) \int d^2\mathbf{k}_{\parallel}^{(0)} \int d^2\mathbf{k}_{\parallel} e^{i\mathbf{k}_{\parallel} \cdot \mathbf{r}_{\parallel}} \hat{\xi}(\mathbf{k}_{\parallel} - \mathbf{k}_{\parallel}^{(0)}) \times \int dz' d_{\mu\nu}(\mathbf{k}_{\parallel}, \omega|zz') \delta(z') \tilde{E}_{\nu}^{(0)}(\mathbf{k}_{\parallel}^{(0)}, \omega|z'). \quad (4)$$

However, since we shall work only in the limit of shallow roughness, we shall further assume that only incident waves with $\mathbf{k}_{\parallel}^{(0)} \approx 0$ will be reflected to the dipole site. Hence, we shall approximate $E_{\nu}^{(0)}$ in Eq. (4) in the form $\tilde{E}_{\nu}^{(0)}(\mathbf{k}_{\parallel}^{(0)}, \omega|z') = E_{\nu}^{(0)}(\omega|z') \delta(\mathbf{k}_{\parallel}^{(0)})$ and by having the dipole located at $\mathbf{r} = (0, 0, d)$, we finally obtain the roughness contribution to the ‘‘parallel components’’ of the reflected field for a point on the z -axis given by

$$E_x^{rR}(z, \omega) = -\frac{k^2}{16\pi^3} [\varepsilon(\omega) - 1] \int d^2\mathbf{k}_{\parallel} \hat{\xi}(\mathbf{k}_{\parallel}) \times \int dz' [d_{xx} E_x^{(0)} + d_{xy} E_y^{(0)} + d_{xz} E_z^{(0)}] \delta(z'), \quad (5)$$

$$E_y^{rR}(z, \omega) = -\frac{k^2}{16\pi^3} [\varepsilon(\omega) - 1] \int d^2\mathbf{k}_{\parallel} \hat{\xi}(\mathbf{k}_{\parallel}) \times \int dz' [d_{yx} E_x^{(0)} + d_{yy} E_y^{(0)} + d_{yz} E_z^{(0)}] \delta(z'). \quad (6)$$

Next we have to calculate the components $E_i^{(0)}$ from the CPS theory for flat surfaces.³ Since our interest is only to evaluate expressions (5) and (6) on the z axis with $(x, y) = (0, 0)$, it is not difficult to verify from the original CPS theory (which applies the Sommerfeld solutions in terms of the Hertz vectors) that for an x -oriented dipole, only $E_x^{(0)}$ survives in Eq. (5) and for an y -oriented dipole, only $E_y^{(0)}$ contributes in Eq. (6). Hence, E_i^{rR} in Eqs. (5) and (6) evaluated at $(0, 0, z)$ will take the following simple forms:

$$E_x^{rR}(z, \omega) = -\frac{k^2}{16\pi^3} [\varepsilon(\omega) - 1] \int d^2\mathbf{k}_{\parallel} \hat{\xi}(\mathbf{k}_{\parallel}) \times \int dz' d_{xx} E_x^{(0)}(z') \delta(z'), \quad (7)$$

$$E_y^{rR}(z, \omega) = -\frac{k^2}{16\pi^3} [\varepsilon(\omega) - 1] \int d^2\mathbf{k}_{\parallel} \hat{\xi}(\mathbf{k}_{\parallel}) \times \int dz' d_{yy} E_y^{(0)}(z') \delta(z'), \quad (8)$$

with $E_i^{(0)} = E_i^{\text{in}} + E_i^{rF}$ and can be expressed in terms of the ‘‘Sommerfeld integrals’’ as given in the CPS paper:³

$$E_i^{\text{in}}(z', \omega) = \hat{e}_i \mu k^3 \int_0^\infty du \frac{u^3}{l_1} e^{kl_1(z'-d)}, \quad (9)$$

$$E_i^{rF}(z', \omega) = \hat{e}_i \frac{\mu k^3}{2} \int_0^\infty du \frac{u}{l_1} [(1-u^2)R^\parallel + R^\perp] e^{-kl_1(z'+d)}. \quad (10)$$

Note that in the case of flat surface, there is *no* distinction between the x -dipole case and the y -dipole case. $R^\parallel = (l_2 - \varepsilon l_1)/(l_2 + \varepsilon l_1)$ and $R^\perp = (l_1 - l_2)/(l_1 + l_2)$ are the Fresnel coefficients with $l_1 = -i\sqrt{1-u^2}$ and $l_2 = -i\sqrt{\varepsilon-u^2}$. Hence the integrals $\int dz'$ in Eqs. (7) and (8) can be evaluated to yield

$$\begin{aligned} & \int dz' d_{xx} E_x^{(0)}(z') \delta(z') \\ &= \frac{\mu k^3}{2} d_{xx}(\mathbf{k}_\parallel, \omega|z, 0) \\ & \times \int_0^\infty du \frac{u}{l_1} [2u^2 + (1-u^2) \\ & \times R^\parallel + R^\perp] e^{-kl_1 d}, \end{aligned} \quad (11)$$

$$\begin{aligned} & \int dz' d_{yy} E_y^{(0)}(z') \delta(z') \\ &= \frac{\mu k^3}{2} d_{yy}(\mathbf{k}_\parallel, \omega|z, 0) \\ & \times \int_0^\infty du \frac{u}{l_1} [2u^2 + (1-u^2) \\ & \times R^\parallel + R^\perp] e^{-kl_1 d}. \end{aligned} \quad (12)$$

Note that since both the dyadics and the components $E_x^{(0)}$ and $E_y^{(0)}$ are continuous across the surface $z=0$, there is no ambiguity in carrying out the integral $\int dz' \delta(z')$ to arrive at Eqs. (11) and (12). In comparison, for the case of a perpendicular dipole, such an integral must be handled with care since $E_z^{(0)}$ is not continuous at the boundary.^{9,14} To proceed further with the calculation, we need the expressions for the Green dyadics from the MM paper which can be obtained as follows:¹³

$$d_{xx}(\mathbf{k}_\parallel, \omega|z, z'=0) = \frac{4\pi i}{k^2 k_\parallel^2} e^{ik_2 z} \left(\frac{k^2 k_y^2}{k_1 - k_2} - \frac{k_1 k_2 k_x^2}{k_1 - \varepsilon k_2} \right), \quad (13)$$

$$d_{yy}(\mathbf{k}_\parallel, \omega|z, z'=0) = \frac{4\pi i}{k^2 k_\parallel^2} e^{ik_2 z} \left(\frac{k^2 k_x^2}{k_1 - k_2} - \frac{k_1 k_2 k_y^2}{k_1 - \varepsilon k_2} \right), \quad (14)$$

where k_1 and k_2 are defined as

$$k_1 = -(\varepsilon k^2 - k_\parallel^2)^{1/2},$$

$$k_2 = \begin{cases} (k^2 - k_\parallel^2)^{1/2}, & k^2 > k_\parallel^2 \\ i(k_\parallel^2 - k^2)^{1/2}, & k^2 < k_\parallel^2. \end{cases} \quad (15)$$

Furthermore, for a sinusoidal grating surface profile with

$$\hat{\zeta}(\mathbf{k}_\parallel) = (2\pi)^2 \zeta_0 \delta(\mathbf{Q} - \mathbf{k}_\parallel), \quad \mathbf{Q} = Q \hat{e}_x, \quad (16)$$

the integrals $\int d^2 \mathbf{k}_\parallel$ in Eqs. (5) and (6) can be evaluated [with the results in Eqs. (11)–(14)] to give

$$\int d^2 \mathbf{k}_\parallel \hat{\zeta}(\mathbf{k}_\parallel) d_{xx}(\mathbf{k}_\parallel, \omega|z) = -i \frac{16\pi^3 \zeta_0}{k^2} \frac{k_1 k_2}{k_1 - \varepsilon k_2} e^{ik_2 z}, \quad (17)$$

$$\int d^2 \mathbf{k}_\parallel \hat{\zeta}(\mathbf{k}_\parallel) d_{yy}(\mathbf{k}_\parallel, \omega|z) = i \frac{16\pi^3 \zeta_0}{k_1 - k_2} e^{ik_2 z}. \quad (18)$$

Substituting Eqs. (11), (12), (17), and (18) into Eqs. (7) and (8), we finally obtain the first-order roughness contribution to the reflected field at the dipole site ($z=d$) in the following form:

$$\begin{aligned} E_x^{rR} &= \frac{i\mu k^3}{2} (\varepsilon - 1) \zeta_0 \frac{k_1 k_2}{k_1 - \varepsilon k_2} e^{ik_2 d} \\ & \times \int_0^\infty du \frac{u}{l_1} [2u^2 + (1-u^2)R^\parallel + R^\perp] e^{-kl_1 d}, \end{aligned} \quad (19)$$

$$\begin{aligned} E_y^{rR} &= -\frac{i\mu k^5}{2} (\varepsilon - 1) \zeta_0 \frac{1}{k_1 - k_2} e^{ik_2 d} \\ & \times \int_0^\infty du \frac{u}{l_1} [2u^2 + (1-u^2)R^\parallel + R^\perp] e^{-kl_1 d}. \end{aligned} \quad (20)$$

III. MOLECULAR FLUORESCENCE CHARACTERISTICS

From the results in the above section, we can hence obtain the modified emission frequency and the decay rate from Eqs. (1) and (2) in the following form:

$$\frac{\Delta\omega}{\gamma_0} = -\frac{3q}{4k^3} \text{Re}G_i, \quad (21)$$

$$\frac{\gamma}{\gamma_0} = 1 + \frac{3q}{2k^3} \text{Im}G_i, \quad (22)$$

where $G_i = E_i^r/\mu$ is the reflected field acted on the dipole per unit dipole moment of the admolecule with the subscript i indicating the orientation of the dipole with respect to the surface. To be complete and self-contained, we give below the full set of solutions for G_i to first-order roughness for a grating surface obtained in both the dynamic and the approximated static image theories. Thus let us write

$$G_i = G_i^F + G_i^R, \quad (23)$$

where G_i^F is given by the CPS theory in the dynamical approach as follows. *For a parallel dipole (for both x and y),*

$$G_{x,y}^F = \frac{k^3}{2} \int_0^\infty du \frac{u}{l_1} [(1-u^2)R^\parallel + R^\perp] e^{-2kl_1d}, \quad (24)$$

for a perpendicular dipole (z),

$$G_z^F = -k^3 \int_0^\infty du \frac{u^3}{l_1} R^\parallel e^{-2kl_1d} \quad (25)$$

G_i^R is then obtained from the results in Eqs. (19) and (20) together with previous results⁹ as follows:

$$G_x^R = \frac{ik^3}{2} (\varepsilon - 1) \zeta_0 \frac{k_1 k_2}{k_1 - \varepsilon k_2} e^{ik_2d} \times \int_0^\infty du \frac{u}{l_1} [2u^2 + (1-u^2)R^\parallel + R^\perp] e^{-kl_1d}, \quad (26)$$

$$G_y^R = -\frac{ik^5}{2} (\varepsilon - 1) \zeta_0 \frac{1}{k_1 - k_2} e^{ik_2d} \times \int_0^\infty du \frac{u}{l_1} [2u^2 + (1-u^2)R^\parallel + R^\perp] e^{-kl_1d}, \quad (27)$$

$$G_z^R = -ik^3 (\varepsilon - 1) \zeta_0 \frac{Q^2}{k_1 - \varepsilon k_2} e^{ik_2d} \int_0^\infty du \frac{u^3}{l_1} (1 - R^\parallel) e^{-kl_1d}, \quad (28)$$

where k_1 and k_2 in Eqs. (26)–(28) are defined as

$$k_1 = -(\varepsilon k^2 - Q^2)^{1/2}, \quad (29)$$

$$k_2 = \begin{cases} (k^2 - Q^2)^{1/2}, & k^2 > Q^2 \\ i(Q^2 - k^2)^{1/2}, & k^2 < Q^2. \end{cases}$$

In the long-wavelength limit, one can also apply the static image theory to obtain the following results:⁸

$$G_x = G_x^F + G_x^R = \frac{(\varepsilon - 1)}{(\varepsilon + 1)} \left(\frac{1}{8d^3} \right) + \frac{4\zeta}{\pi} \frac{\varepsilon - 1}{(\varepsilon + 1)^2} \times \int_0^\infty du \int_0^\infty dv \frac{u^2 - \frac{Q^2}{4}}{fg} (\varepsilon fg + h) \exp[-(f+g)d], \quad (30)$$

$$G_y = G_y^F + G_y^R = \frac{(\varepsilon - 1)}{(\varepsilon + 1)} \left(\frac{1}{8d^3} \right) + \frac{4\zeta}{\pi} \frac{\varepsilon - 1}{(\varepsilon + 1)^2} \times \int_0^\infty du \int_0^\infty dv \frac{v^2}{fg} (\varepsilon fg + h) \exp[-(f+g)d], \quad (31)$$

$$G_z = G_z^F + G_z^R = \frac{\varepsilon - 1}{\varepsilon + 1} \left(\frac{1}{4d^2} \right) + \frac{4\zeta}{\pi} \frac{\varepsilon - 1}{(\varepsilon + 1)^2} \times \int_0^\infty du \int_0^\infty dv (\varepsilon fg + h) \exp[-(f+g)d], \quad (32)$$

where f, g, h are functions of u, v , given by

$$f(u, v) = [(u + Q/2)^2 + v^2]^{1/2},$$

$$g(u, v) = [(u - Q/2)^2 + v^2]^{1/2},$$

$$h(u, v) = u^2 + v^2 - Q^2/4.$$

Another limiting case of interest is the perfect reflecting (conducting) limit in which both the Fresnel coefficients R^\parallel and R^\perp are set to -1 .³ For flat substrate surfaces, this case was considered in the original works by CPS and others for both the parallel and perpendicular dipoles. It is therefore tempting for us to study the same limiting case for rough surfaces following the above formulation as was done for the case of perpendicular dipoles in one of our previous works.¹¹ However, on a careful reexamination, we find that this is illegitimate in the present approach since we believe that the original MM perturbation theory¹³ to lowest order is valid only for the case when the roughness amplitude ζ is much less than the skin depth of the substrate metal. This can be seen from the original expansion of the dielectric function $\varepsilon(z, \omega)$ in terms of ζ in the MM paper [Eq. (2.3) of Ref. 13] in which the expansion will lose meaning for a perfect conducting substrate with $\text{Re}(\varepsilon) \rightarrow -\infty$. Thus, for a perfect conductor with a zero skin depth, the perfect reflecting limit cannot be taken in our present perturbation theory for rough surfaces as was mistakenly done in our previous work.¹⁵ So it seems that for the perfect reflecting limit, which is a relatively simple case with a flat substrate surface, the molecular fluorescence properties must be studied nonperturbatively in the case with a rough surface.¹⁶

IV. RESULTS AND DISCUSSION

We have applied the above theory of interaction between an emitting dipole and a periodic conducting surface to compute the fluorescence characteristics of molecules at a grating surface: the x orientation being that in which the dipole is oriented along the direction of the grating, the y orientation with the dipole situated parallel to the grooves, and the z orientation with the dipole perpendicular to the substrate. Figure 1 shows the geometry of the system. Listed are the dipole-substrate distance d , the roughness parameters ζ_0 (amplitude) and Q (period), and the dielectric constants of the substrate, $\varepsilon(\omega)$, with the dipole located in a vacuum. All the computations were carried out in the limit of shallow roughness with $Q\zeta_0 = 0.02$ and the substrate taken as silver whose optical properties can be obtained from the literature.¹⁷ Figure 2 shows the comparison of the static and dynamic theories by plotting the imaginary part of the roughness contribution, $\text{Im } G^R$, against the distance d for the three dipole orientations. It can be seen that for the y and z orientations, the two theories compare well at close distances, while at greater distances, the static (image) theory is consistently below that of the dynamical theory. This observation is in agreement with previous work for flat surfaces¹⁸ and vertical dipoles at grating surfaces.⁹ However, the x orientation differs from the other two in that the dynamic theory gives negative values for $\text{Im } G^R$ at close distances. The displayed graphic was offset by a constant so it could be shown on a logarithmic plot. We believe the dramatic difference in the x orientation has its origin from the radiative transfer

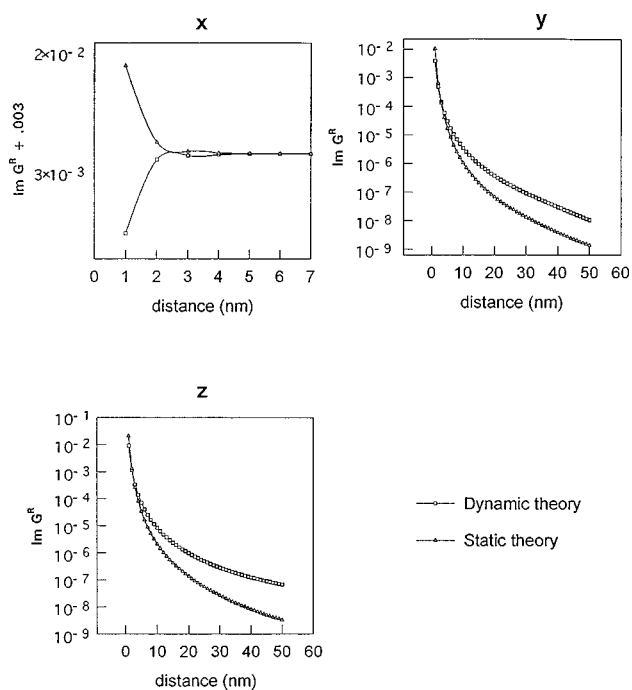


FIG. 2. Comparison between the static and dynamic theories by plotting $\text{Im } G^R$ in Eqs. (26)–(28) and in Eqs. (30)–(32) as a function of the dipole-substrate distance. The labels x , y , and z indicate the three orientations of the molecule.

between the molecule and the surface which can only be accounted for in a dynamic theory.¹² It is well known that the distance dependence of the decay rates for the case of flat surfaces is highly sensitive to the molecular orientation, due mainly to the predominance of radiative transfer at relatively far distances for the perpendicular dipoles but much less for the parallel dipoles.³ In the presence of roughness, this issue is further complicated by the fact that nonradiative transfer can be transformed back to a radiative one due to the recoupling of evanescent surface modes to radiative modes. This recoupling mechanism is particularly significant for the x dipole being oriented along the direction of the grating wave vector.

Figure 3 shows the results obtained for the decay rate at a rough surface, normalized to the flat surface values, as a function of distance. The curves have varying emitting frequencies and they all tend to unity at far distances as expected. At closer distances ($d \leq 25$ nm), the results are sensitive to both the dipole orientation and the emission frequency. The most interesting observation from these is that the presence of roughness can both enhance or suppress the flat surface decay rates for ad molecules, in agreement with previous remarks^{8,9,12} and is somewhat unexpected from other investigations.⁷ Specifically, we note that within this frequency range, the grating roughness tends to decrease the flat surface decay values for the x -oriented dipoles while enhancing those for the y - and z -oriented dipoles. In general, both enhancement and diminution can occur for all the x , y , and z dipoles at different emission frequencies.

Having studied the effect of the roughness with respect to a flat surface, we shall for the rest of our calculation simply normalize the emission characteristics in the presence of the grating with respect to those for a free molecule. Figure 4

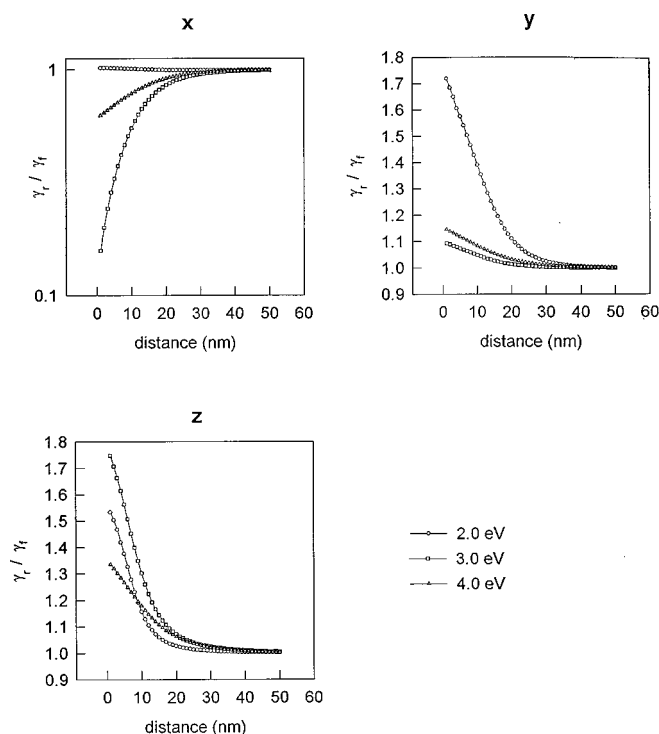


FIG. 3. Ratio of the decay rate at rough surface to that at flat surface as a function of distance, plotted for three different emission frequencies.

shows the total (“flat+rough”) decay rate normalized to that of a free molecule. We notice that while the perpendicular (z) dipole always has its surface-induced decay rate greater than that of a free molecule, the parallel (x and y) dipoles

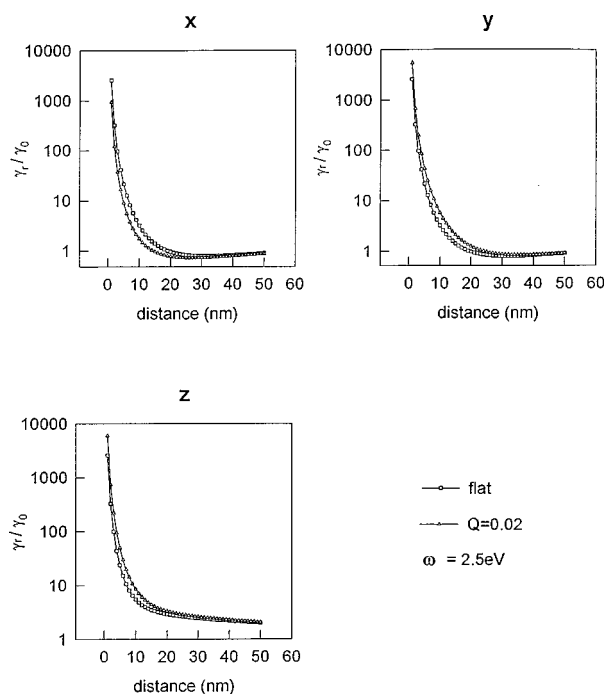


FIG. 4. Similar to Fig. 3, except the surface-induced decay rate is normalized to the free molecule value, rather than to the flat surface value. The case for a flat surface and that for a grating with $Q=0.02 \text{ nm}^{-1}$ are shown for the emission frequency at 2.5 eV.

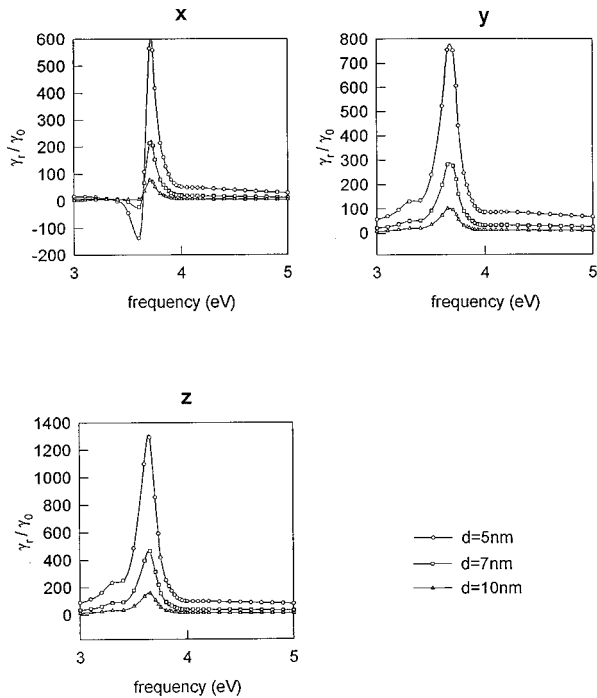


FIG. 5. Normalized decay rate spectrum for a grating surface with $Q=0.02 \text{ nm}^{-1}$ as a function of emission frequency at three different molecule-surface distances.

can have the induced rates less than the free molecule rate at relatively far distances. This is well known with flat surfaces and is due again to the aforementioned relatively small radiative transfer for parallel dipoles at far distances as a result of the “destructive interference effect” between the radiating dipole and its image.³ However, in the presence of roughness, the x dipole has its decay rate less than the flat surface values since the roughness contribution is negative (see Fig. 2) while the y dipole behaves just the opposite. This leads to the result that the total decay rate for the x dipole at a grating surface can become *smaller* than the free molecule rate at *closer* distances (reduced from about 20 nm to 10 nm) from the surface. The result will be somewhat dramatic if the drop below the free molecule rate can occur at even closer distances (say, $d \leq 5$ nm) within which the presence of the surface is traditionally thought to certainly increase the damping of the molecule due to nonradiative transfer. Although we cannot demonstrate this from our present perturbative calculation, our result surely leaves open the possibility that the presence of roughness can be exploited to lengthen the lifetimes of the admolecules (even beyond its free molecule value) by manipulating the orientations of the molecules. This possibility will have significant implications to performing photochemistry at rough metallic surfaces.¹²

Figure 5 shows the same total decay rate as a function of emission frequencies. It should be pointed out that there exists *two* “resonance structures” in our perturbative formalism as can be seen from Eqs. (26)–(28). One structure depends on the presence of the roughness (the morphology- or Q -dependent resonance) as can be seen from the terms $\sim 1/(k_1 - \epsilon k_2)$ or $\sim 1/(k_1 - k_2)$. The other is just like the flat surface case through the factors R^\perp and R^\parallel which imply a surface plasmon resonance at about 3.7 eV for a silver substrate. These two structures interplay with each other in a

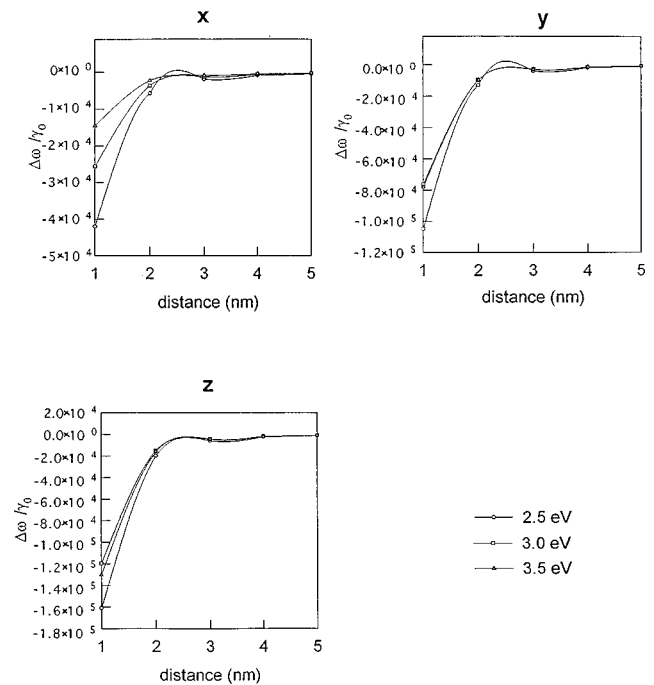


FIG. 6. Normalized molecular frequency-shifts for a grating surface with $Q=0.02 \text{ nm}^{-1}$ as a function of distance for three different emission frequencies.

complicated manner depending on the value of Q , the distance, as well as the molecular orientation. As a result, a kind of “shoulder peak” is manifested in some of these plots.¹⁰ We believe that the negative results for the x dipoles at close distances are unacceptable and reflect once again the limitation of the present perturbative approach.

The remaining two graphs show the result for frequency-shift calculations for different molecular orientations. Aside from the general surface-induced redshifts appreciable at close distances and low emission frequencies as observed before,¹¹ we also notice the following interesting features. Figure 6 shows the shifts as a function of distance for three different emitting frequencies. We notice that while the x dipole has in general smaller redshifts in its frequency, it is also more sensitive to the change of emitting frequency as compared to the cases with the y and z dipoles. Furthermore, it is interesting to note that the surface effects on the emission frequency drop down much more rapidly than as in the case for the decay rates as the molecule is located farther away from the surface. Figure 7 shows the result as a function of the emission frequency at a fixed distance $d = 10$ nm. Again, we see the extra Q -dependent resonance structure showing up for values of k close to Q ($Q = 0.02 \text{ nm}^{-1}$) in the case of the x and z dipoles. The disappearance of the effect at high emission frequencies probably has to do with the “overall cancellation” of the contributions due to the misaligned image dipoles which become more significant when the source dipole oscillates very rapidly.

We emphasize again that all the above numerical conclusions are obtained to lowest order from the perturbation theory formulated in Sec. II and III. As pointed out in different places in the above, the accuracy of this theory is limited to (1) small surface roughness, i.e., $\zeta_0 \leq 1/Q$ for a grating surface and (2) relatively low dynamic conductivity

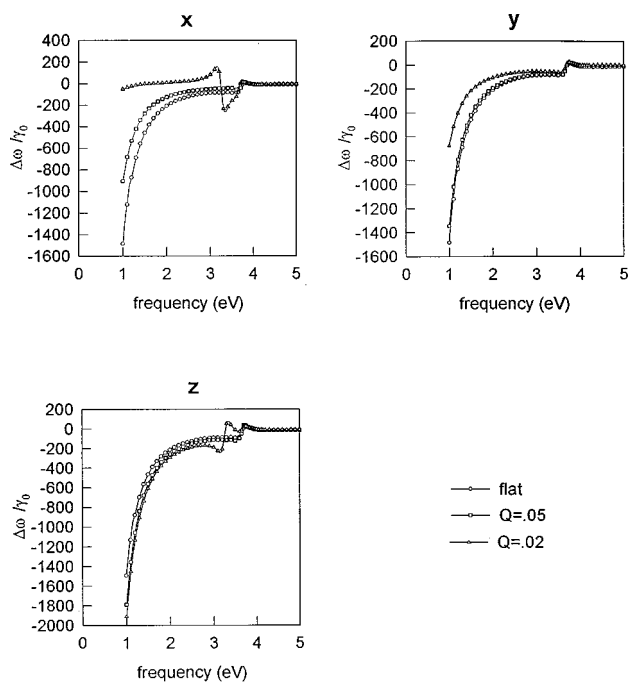


FIG. 7. Same as in Fig. 6, except for a plot as a function of emission frequencies at a fixed distance of 10 nm. The results are shown for a flat, grating surface with $Q=0.02 \text{ nm}^{-1}$, and one with $Q=0.05 \text{ nm}^{-1}$, respectively.

of the metal, i.e., $\zeta_0 \lesssim \delta$, the skin depth of the metal. Furthermore, since we did not include a full 2D Fourier transform for the incident dipolar field as discussed in Sec. II, we expect the results are more accurate at farther molecule-surface distances, though we have to be reminded that the roughness effects become very insignificant when the molecule is too far away (Fig. 3). Given the above summary, we believe that it is hopeful for experiments to be designed to test and to go beyond the results from the present modeling.

V. CONCLUSION

The dynamical theory for the effects on dipole emission near a rough conducting substrate has been expanded to include cases where the dipole has parallel and perpendicular orientations. We have explored the possible effects as functions of dipole distance from the substrate, dipole emission frequency, dipole orientation, and surface roughness. We have seen that small changes in these parameters can affect the decay rate and frequency shift in most cases. Although our present theory is limited by its perturbative approach and other shallow-roughness approximations, we have illustrated the importance of establishing a dynamic theory for this phenomenon, with the hope that in the future more accurate (e.g., nonperturbative) approaches will become available. Among other results as already elaborated in the above section, we stress that our present study implies an important modification in the usual step that people take to compare experimental and theoretical results by “averaging” the theoretical calculated values over the orthogonal molecular orientations. For example, for decay rate (γ) calculations, it is a common practice to compare $\gamma \equiv \gamma_{\perp}/3 + 2\gamma_{\parallel}/3$ with experimental measurements. However, for patterned surfaces, our result shows that it may be more reasonable to compare the measurements with the calculated $\gamma \equiv (\gamma_x + \gamma_y + \gamma_z)/3$. Furthermore, it will also be interesting if future experimental evidence can indeed demonstrate the possibility of exploiting patterned surface roughness to lengthen the molecular lifetimes relative to those of a free molecule as well as those of a flat substrate surface.

ACKNOWLEDGMENTS

We thank Matthew Hider for discussion and the Faculty Development Grant of Portland State University for partial support of the present work.

*Author to whom correspondence should be addressed.

¹H. Kuhn, *J. Chem. Phys.* **53**, 101 (1970).

²K. H. Drexhage, in *Progress in Optics XII*, edited by E. Wolf (North-Holland, Amsterdam, 1974), p. 165ff.

³R. R. Chance, A. Prock, and R. Silbey, *Adv. Chem. Phys.* **37**, 1 (1978).

⁴R. Rossetti and L. E. Brus, *J. Chem. Phys.* **73**, 572 (1980); **76**, 1146 (1982); A. P. Alivisatos, D. H. Waldeck, and C. B. Harris, *ibid.* **82**, 541 (1985).

⁵For more recent reviews, see, e.g., D. H. Waldeck, A. P. Alivisatos, and C. B. Harris, *Surf. Sci.* **158**, 103 (1985); R. R. Cavanagh, E. J. Heilweil, and J. C. Stephenson, *ibid.* **299/300**, 643 (1994).

⁶A. Sommerfeld, *Ann. Phys. (Leipzig)* **28**, 665 (1909); **81**, 1135 (1926).

⁷J. Arias, P. K. Aravind, and H. Metiu, *Chem. Phys. Lett.* **85**, 404 (1982).

⁸P. T. Leung, Z. C. Wu, D. A. Jelski, and T. F. George, *Phys. Rev. B* **36**, 1475 (1987).

⁹P. T. Leung and T. F. George, *Phys. Rev. B* **36**, 4664 (1987).

¹⁰P. T. Leung, Y. S. Kim, and T. F. George, *Phys. Rev. B* **38**, 10 032 (1988).

¹¹M. H. Hider and P. T. Leung, *Phys. Rev. B* **44**, 3262 (1991).

¹²For recent review, see, e.g., P. T. Leung and T. F. George, *J. Chim. Phys. Phys.-Chim. Biol.* **92**, 226 (1995).

¹³A. Maradudin and D. L. Mills, *Phys. Rev. B* **11**, 1392 (1975).

¹⁴G. S. Agarwal, *Phys. Rev. B* **14**, 846 (1976).

¹⁵The results for a perfect conducting substrate presented in Ref. 11 are wrong [i.e., Eq. (6) and Figs. 4 and 5]. The factor $(\epsilon - 1)/(k_1 - \epsilon k_2)$ appearing in Eq. (6) should also have been considered in the perfect conducting limit.

¹⁶See, e.g., the recent article by A. A. Maradudin, A. V. Shchegrov, and T. A. Leskova, *Opt. Commun.* **135**, 352 (1997), for the treatment of light scattering, and references therein.

¹⁷*Handbook of Optical Constants of Solids*, edited by E. D. Palik (Academic, New York, 1985), Vol. 1.

¹⁸P. T. Leung, T. F. George, and Y. C. Lee, *J. Chem. Phys.* **86**, 7227 (1987).